



# Physics-based modeling of metal additive manufacturing processes: a review

Shuozhi Xu<sup>1</sup> · Mohammad Younes Araghi<sup>1</sup> · Yanqing Su<sup>2</sup>

Received: 22 May 2024 / Accepted: 16 July 2024 / Published online: 30 July 2024  
© The Author(s), under exclusive licence to Springer-Verlag London Ltd., part of Springer Nature 2024

## Abstract

In the modern world, the ubiquity and critical importance of metallic materials are evident in everything from infrastructure and transportation to electronics and aerospace. Additive manufacturing (AM) of metals has revolutionized traditional production methods by enabling the creation of high-value components with topologically optimized complex geometries and functionalities. This review addresses the critical need for sophisticated physics-based models to investigate and optimize the AM processes of metals. We explore both melt-based and solid-state AM techniques, highlighting the current state-of-the-art modeling approaches. The purpose of this review is to evaluate existing models, identify their strengths and limitations, and suggest areas for future research to enhance the predictability and optimization of AM processes. By summarizing and comparing various modeling techniques, this review aims to provide a comprehensive understanding of the current research landscape. We focus on the pros and cons of different models, including their applicability to key elements and processes common to both melt-based and solid-state AM methods. Where multiple models exist for a single technique, a comparison is drawn to highlight their relative pros and cons. Concluding this review, we contemplate prospective advancements in sophisticated physics-based process modeling and strategies for their integration with models for structure-properties relations.

**Keywords** Additive manufacturing · Physics-based modeling · Metallic materials

## 1 Introduction

The evolution of metallic materials has been a cornerstone of societal progress, marking significant leaps from the Bronze Age to today's high-tech alloys, each transition underpinning advancements in technology and industry [1]. Achieving the urgent societal goals of reduced emissions and increasing energy efficiency is driving the development of novel metals with unprecedented performance [2]. One path is lightweight metals (e.g., Al and Mg) for room-temperature applications such as infrastructure and transportation [3]. A second path is ductile metals at low or cryogenic temperatures (e.g., stainless steels and Ti alloys) for high-latitude vessels and Arctic pipelines [4]. The third path is high-temperature damage-tolerant metals (e.g., superalloys and metallic glasses) for

aircraft engines and nuclear reactors where the thermal efficiency generally increases with the operating temperature [5]. Many of these metals can be produced by additive manufacturing (AM), which makes objects from 3D model data, usually layer upon layer, as opposed to subtractive methodologies where objects are formed by removing materials through cutting, drilling, milling, or grinding [6]. AM is advantageous over subtractive manufacturing in that high-value component with topologically optimized complex geometries and functionalities become achievable [7]. Therefore, metal AM (MAM) has the potential to improve the sustainability of key industrial sectors, eliminate several energy-intensive fabrication steps, and reduce raw material requirements [8]. In the meantime, it can produce parts with mechanical properties that are comparable or superior to the traditionally manufactured ones [9].

There are two main types of MAM: melt-based and solid-state [10]. MAM has many advantages, including the freedom to create complex geometries, the ability to process hard-to-machine materials, and the ability to manufacture functional prototypes directly for use. Despite this, there

✉ Shuozhi Xu  
shuozhixu@ou.edu

<sup>1</sup> School of Aerospace and Mechanical Engineering, University of Oklahoma, Norman 3019-1052, OK, USA

<sup>2</sup> Department of Mechanical and Aerospace Engineering, Utah State University, Logan 4322-4130, UT, USA

are several challenges associated with the melt-based MAM, including high residual stresses, significant thermal gradients, and defects such as porosity and hot cracking caused by melting and rapid solidification [11, 12]. It is possible that these issues can adversely affect the mechanical properties and dimensions of the fabricated parts. In the meantime, solid-state AM processes do not melt the material, thereby reducing residual stresses and defects resulting from phase changes [13]. However, solid-state AM is not without its own challenges, which include limited material choices and difficulty achieving high-density parts. As a general rule, while solid-state AM reduces thermal problems, melt-based AM offers greater versatility when it comes to materials and part complexity [14].

Given the challenges and high costs of preparing feed materials and operating MAM machines [15], utilizing physics-based models to study the MAM process has become increasingly popular [16]. Several reviews have focused on the physics-based modeling of melt-based MAM techniques [17–22], while much fewer have addressed solid-state methods [23]. As a result, we provide here a short review to summarize mainstream physics-based models in most, if not all, MAM processes. This review is unique because it focuses on the pros and cons of different models for important elements or processes, some of which are common between the melt-based and solid-state approaches. A list of open-source software packages is also provided for each model.

## 2 Classification

There are two types of melt-based MAM methods: powder bed fusion (PBF) and directed energy deposition (DED) [24]. PBF uses a laser or electron beam to selectively melt and fuse powder materials layer by layer within a confined bed area [25]. On the other hand, DED involves no bed but instead feeds powders or wires directly into a focused energy source, such as a laser beam, an electron beam, or an arc, which melts the metal as it is deposited on the build surface or an existing part [26]. Between the two types of feed materials, wires have a higher deposition efficiency with less waste, while powders have greater material variety and are better for com-

plex geometries [27]. PBF is renowned for its high precision and the ability to create complex internal shapes, while DED stands out for its rapid material deposition capabilities and its proficiency in repairing or adding to existing parts [28]. In both approaches, compared with the laser beam, the electron beam offers deeper material penetration and faster build rates but requires operation under vacuum conditions and may not be optimal for metals that are prone to adverse effects from electron scattering [29]. A summary of different types of melt-based MAM techniques is provided in Fig. 1.

There are four types of solid-state AM methods: cold spray, field-assisted AM, friction-based AM, and binder jetting [30]. The cold spray uses a high-velocity gas jet to accelerate metal particles onto a substrate, creating a coating or part without significant heating [31]. Working at room temperature, it preserves the original material properties and avoids thermal distortion. Field-assisted AM employs electric, magnetic, acoustic, shear, and/or thermal fields to facilitate the bonding of powders, foils, plates, or wires [32]. It can process a wide range of metals, including difficult-to-sinter ones. Friction-based AM, such as friction welding, generates heat through mechanical friction to join metals [33]. Because the metal is refined, the produced parts can have excellent mechanical properties. Binder jetting deposits a liquid binding agent onto layers of powder metal, bonding these layers together to form a part [34]. It is material-efficient and suitable for complex geometries without support structures. An overview of the various solid-state AM techniques is offered in Fig. 2.

## 3 Feedstock models

### 3.1 Powder

One of the most popular types of feedstock in either melt-based or solid-state AMs is the powder. For example, in PBF and powder-based DED, respectively, powder spreading and powder feeding are the first step and significantly influence

**Fig. 1** Different types of melt-based MAM methods

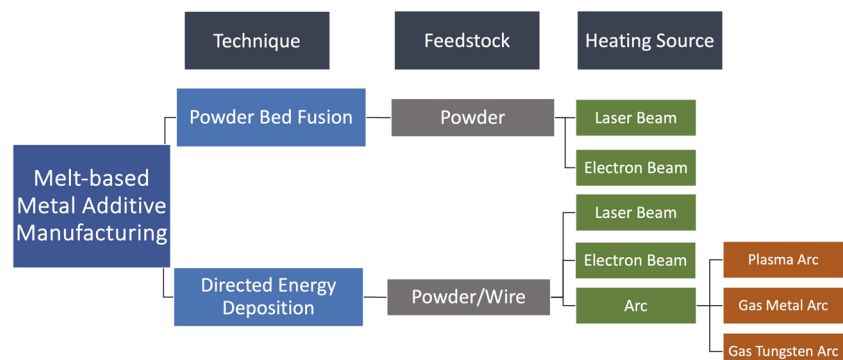
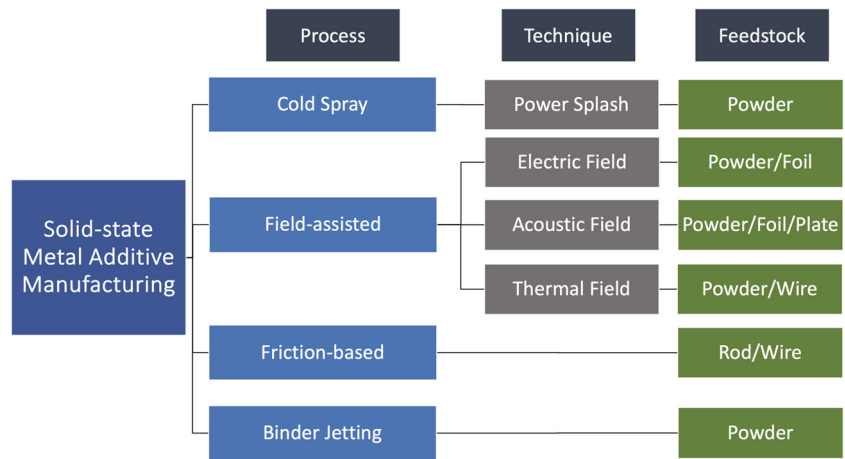


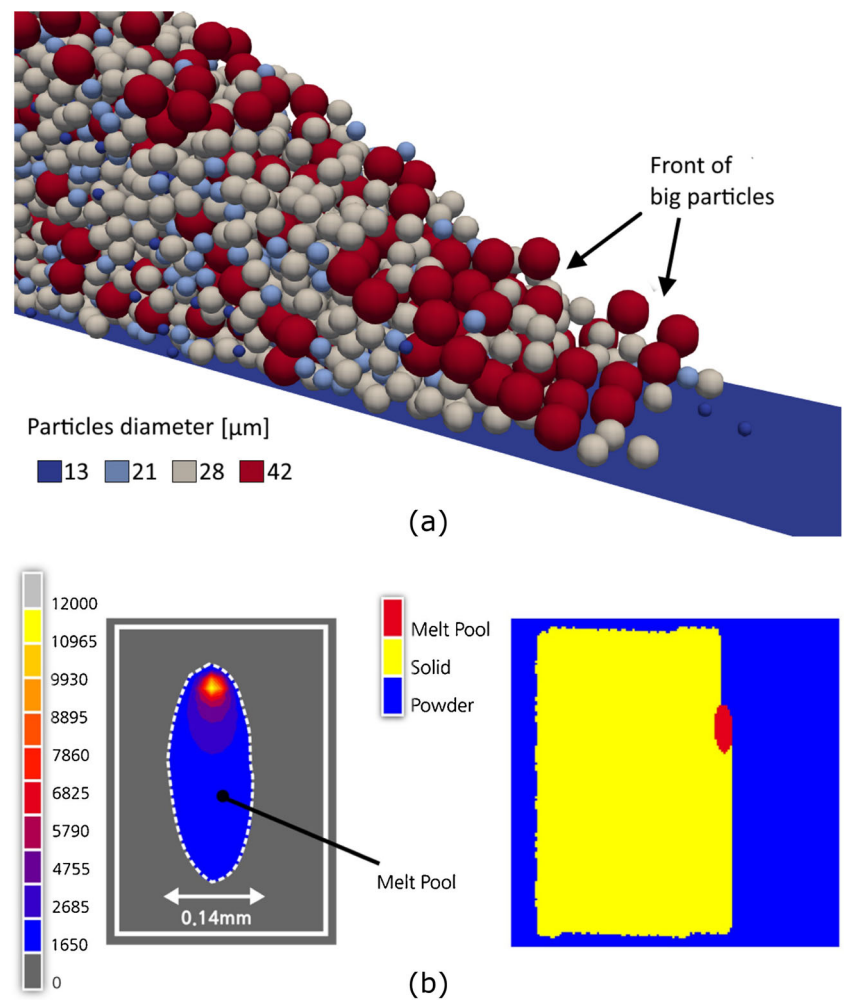
**Fig. 2** Different types of solid-state MAM methods



the subsequent melting process [35]. Powder dynamics also play an important role in cold spray [36], field-assisted AM [37], and binder jetting [38], as long as the feedstock is powder. For a given metal, factors relevant to powder dynamics include but are not limited to powder shape, powder size, powder layer thickness, powder feeding rate, rake shape,

and rake speed. There are mainly two views of the powders: discrete and continuum, as shown in Fig. 3. In the discrete view, cubic arrangements [39] and particle deposition [40] have been employed to simplify the powder bed. However, the most popular method is the discrete element method (DEM) [41], because it accurately simulates individual par-

**Fig. 3** **a** Discrete and **b** continuum treatments, respectively, of the powder bed. In **b**, temperature is in units of °C. **a** is reproduced from Ref. [47], which is under CC BY. **b** is reproduced with permission from Ref. [48]



particle interactions, including contact mechanics, cohesion, and adhesion. DEM's ability to handle non-spherical particles and dynamically track their behavior allows for realistic simulations of powder flow, crucial for optimizing machine design and process parameters [42]. In the continuum view, the powder is treated as a granular flow. As such, common fluid models such as the computational fluid dynamics (CFD) method [43], the lattice Boltzmann method (LBM) [44], and the smoothed particle hydrodynamics (SPH) method [45] can be applied. However, one shortcoming of approximating the powders as a continuous fluid is that it fails to accurately capture collision, friction, and interlocking between particles, which are critical in determining the realistic behavior of powder deposition and spreading in MAM processes [46].

A powder model can be calibrated by adjusting the physical properties of particles such as shape, size, cohesion, friction, and inter-particle forces, to align the model's predictions of powder behavior and flow characteristics with experimental observations [49].

Nine open-source DEM software packages were recently reviewed by Dosta et al. [50]. It was found that while each can handle selected case studies with similar initial setups yielding comparable results, variations are mostly due to differences in the implementation of contact models, particularly the treatment of tangential forces in particle-wall interactions, and the sensitivity of results in penetration tests. As of July 2024, DEM software packages that are being actively developed include GranOO [51], Kratos Multiphysics [52], MercuryDPM [53], MUSEN [54], and Yade [55].

### 3.2 Other feedstocks

In addition to powders, other feedstocks in MAM include wires, rods, plates, sheets, and foils. In melt-based methods, the only non-powder feedstock is wire which is used in some DED processes, e.g., wire arc AM (WAAM). When simulating the WAAM process, the wire itself is usually not explicitly modeled [56]; instead, only results of the heat/wire interactions, e.g., thermal energy or melt, are considered. In solid-state AMs, deformation of the non-powder feedstocks is mainly described by continuum models such as SPH or finite element method (FEM) due to their ability to simulate complex structural behaviors and mechanical interactions under various loading conditions especially severe plastic deformation. For example, a rod in additive friction stir-deposition (AFS-D) processes has been modeled using SPH [57, 58]. Overall, there are much fewer modeling studies of non-powder feedstocks compared with powders in the literature.

## 4 Melting

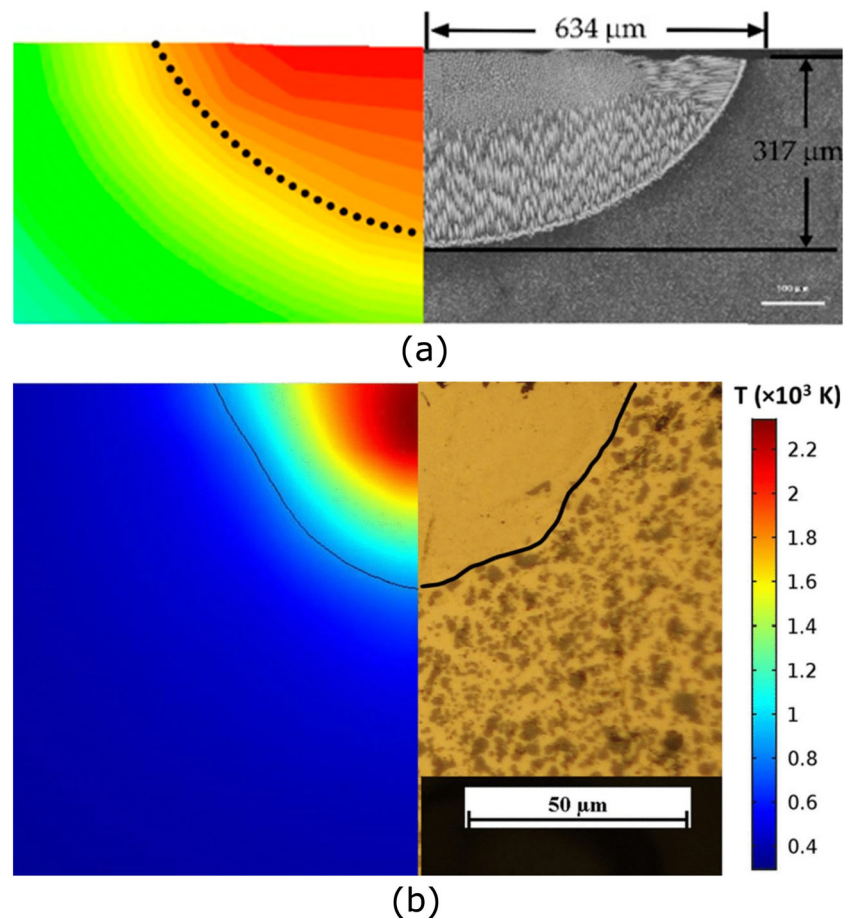
Once the feedstocks are in place, they are selectively melted by a heat source in melt-based MAM. Therefore, modeling melting is relevant only in melt-based MAM, not in solid-state one. The melt pool behavior in MAM is complicated because the interaction between the beam and the metallic powder or wire introduces variables such as the Marangoni effect, evaporation, and denudation zones [59]. The processing parameters can significantly influence the melt pool behavior [60]. Take the PBF as an example. When the laser or electron beam power is too high, deep penetration is created in the melt pool resembling a keyhole shape [61]; when the heat power is too low, the powder particles are insufficiently melted, leading to poor bonding between particles and layers, known as lack of fusion [62]. In addition, thermal gradients within the melt pool result in various solidification rates, residual stresses, and potential defects like porosity or microcracks, making precise control challenging [63].

In the literature, different CFD techniques such as FEM [64], LBM [65], and SPH [66], the finite volume method (FVM) [67], and the level set method [68], have been employed for melting. Two examples are shown in Fig. 4. Each of these methods brings distinct advantages when applied to the melting process of MAM. For example, LBM is good at handling complex boundary interactions, making it efficient for modeling the rapid dynamics [69]; as a mesh-free method, SPH can well handle the free-surface flows and large deformations occurring in the melt pool [70]. However, they may face specific challenges too. For instance, FVM may struggle with capturing sharp interfaces such as those between solid and liquid metals without adequate mesh refinement [71]; LBM may fail to capture the phase change phenomena due to the inherent simplifications in its collision model.

Two phenomena that are closely intertwined with melting are heat transfer and evaporation. The former is related to one unique characteristic of melt-based MAM — high thermal gradient [74]; the latter affects the size, shape, and stability of the melt pool while altering the heat and chemical composition in the molten metal [75]. Thus, melting, heat transfer, and evaporation are strongly coupled, necessitating their simultaneous resolution. All five CFD techniques mentioned earlier can be coupled with additional equations to model heat transfer and evaporation [76]. However, their efficacy in capturing key physical phenomena varies. For instance, FVM is perhaps the best-suited because it conserves mass, momentum, and energy effectively, making it ideal for addressing the interactions among fluid flow, thermodynamics, and mass loss [77]. Meanwhile, typical implementations of SPH struggle to accurately simulate mass transfer and sharp interfaces, rendering it less ideal for modeling evapo-



**Fig. 4** Laser-induced melt pool modeled by **a** FVM and **b** FEM, respectively, compared with experiments. **a** is reproduced from Ref. [72], which is under CC BY. **b** is reproduced with permission from Ref. [73]



ration without significant modifications to the code [78]. On another note, regardless of the chosen CFD technique, the melting model should be integrated with the powder dynamics model (e.g., DEM) [79] to simulate related phenomena such as powder spattering [80].

A melting model can be calibrated by modifying thermal properties, energy input parameters, and phase change characteristics to ensure its predictions of melt pool geometry match experimental observations [81].

There are many CFD software packages that, when combined with appropriate heat transfer and evaporation models, can be applied to the melting process in MAM. Some open-source, general-purpose CFD software packages have been customized specifically for MAM. For example, additiveFOAM [82], developed at the Oak Ridge National Laboratory, is based on OpenFOAM [83] and utilizes FVM. Similarly, researchers at the Los Alamos National Laboratory developed TruchasPBF [84], which is based on Truchas [85] and also employs FVM. In other cases, software was applied to MAM without significant modification, for example, FEniCS [86] (which uses FEM), Palabos [87] (which uses LBM), and DualSPHysics [88] (which uses SPH).

## 5 Solidification

As the heat source moves away, the molten metal solidifies. Thus, like melting, modeling solidification is not relevant in solid-state MAM, but only in melt-based one. During the solidification, key microstructural characteristics such as grain boundaries and cracks emerge. Hence, solidification directly influences the microstructure of the printed metals [89], which in turn dictates their mechanical properties such as strength, toughness, and fatigue resistances [90]. The rapid cooling rates typical of MAM can lead to non-equilibrium microstructures, such as fine grains and metastable phases, which may enhance material properties but also introduce anisotropy and residual stresses [91]. Accurately modeling solidification is thus essential for predicting and controlling these microstructural features and ensuring the structural integrity and performance consistency of the final product [92]. Moreover, understanding solidification patterns allows for the optimization of process parameters to minimize defects such as unwanted porosity and cracking, thereby enhancing the reliability and efficiency of the MAM process [93].

The initial and boundary conditions, e.g., thermal gradients and cooling rates, for solidification modeling are usually provided by the melting simulation. Simple solidification models, such as those based on the volume-of-fluid (VOF) method [96], can distinguish between fluid and solid phases. However, these models do not account for the microstructure of the solid phase. Three numerical methods most commonly applied to microstructure modeling during solidification in MAM, in order of decreasing computational complexity, are: the phase-field (PF) method, kinetic Monte Carlo (kMC), and cellular automata (CA) [89]. Examples based on the PF and CA methods are shown in Fig. 5. PF is adept at handling the diffuse interface between phases and capturing the complex morphologies of solid-liquid interfaces without the need

for tracking or remeshing [97]. Nonetheless, the accuracy of PF simulations is highly dependent on the choice of input parameters, which can be difficult to determine and requires extensive calibration against experimental or higher-fidelity simulations. kMC can effectively handle complex reaction mechanisms and is adaptable to varying conditions, making it useful for exploring different solidification scenarios [98]. However, due to its stochastic nature, kMC can introduce statistical noise into the results, requiring multiple simulations or larger sample sizes to achieve reliable outcomes. The last method, CA, is particularly effective at modeling the microstructures of materials, allowing detailed visualization and analysis of grain growth and orientation during solidification [99]. Nevertheless, CA often simplifies complex physical phenomena into discrete states, which can limit its accuracy in predicting continuous physical changes and interactions. All three methods require thermodynamic data as inputs to accurately simulate the microstructural evolution during solidification. For pure metals, simple data such as melting point and latent heat of fusion are sufficient [100]. For binary alloys, the solidification path can be pre-determined from the phase diagram [101]. For multi-component alloys, however, the use of thermodynamic software becomes necessary because the complexity of interactions among multiple elements requires detailed calculations of phase equilibria and thermodynamic properties across a range of temperatures and compositions [102].

A solidification model can be tuned by altering material properties and processing conditions to ensure its predictions of microstructural evolution and the final structure conform to experimental observations [103].

Many open-source software packages based on PF, kMC, or CA can be directly employed or adapted to simulate microstructural evolution in MAM. For example, Tusas [104] and AMPE [105], both of which are based on the PF method, have been employed for the subgrain scale solidification. SPPARKS [106], which was originally designed for atomic-scale kMC simulations, has been extended to micro-scale solidification. Based on the CA method, ExaCA [94] was developed for CA simulations on exascale supercomputers.

## 6 Late-time microstructural evolution

In melt-based MAM and some solid-state MAM processes that involve heat (e.g., AFS-D), solid-solid phase transformations occur during cooling or heating [107]. For example, in PBF, the previously solidified grains may experience re-growth as they are re-heated when powders above are being scanned [108]. The same phenomena can also manifest during post-build heat treatments, which are frequently

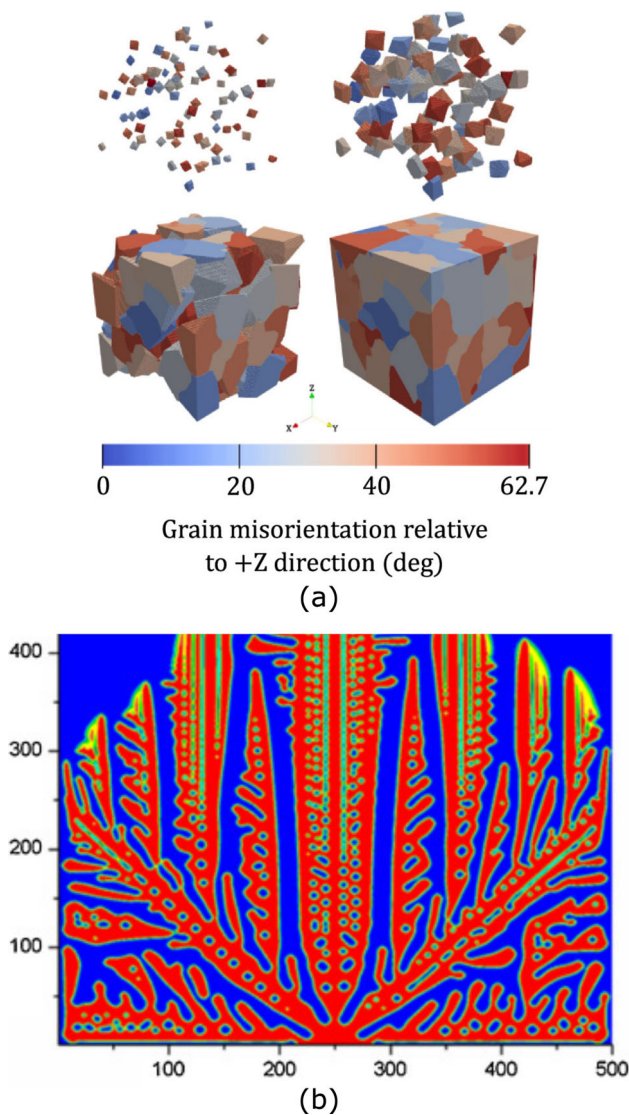


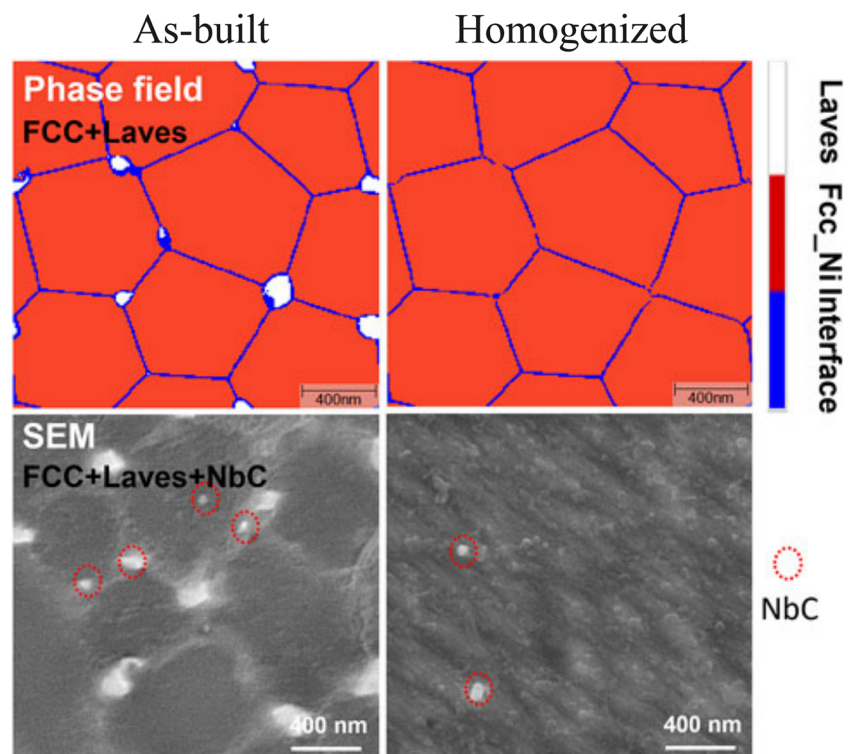
**Fig. 5** Solidification modeled by **a** CA and **b** PF methods, respectively. In **b**, the edge lengths are in units of  $0.2\mu\text{m}$ . Reproduced with permission from Refs. [94, 95]

required when the “as-built” microstructure through melt-based MAM does not satisfy the targeted property specifications [109]. For instance, in precipitation-hardened alloys, the rapid cooling rates associated with laser PBF typically preclude the possibility of diffusion-based precipitation reactions [110]. Consequently, a post-build heat treatment, such as annealing or aging, is essential to facilitate the precipitation of strengthening phases. An example is displayed in Fig. 6. Both *in situ* and post-build solid-solid phase transformations are collectively called “late-time” microstructural evolution. Since the physics at this stage is similar to the microstructural evolution in solidification, all three methods — PF, kMC, and CA — are theoretically applicable. For example, the PF method, using MEUMAPPS-SS [111], has been applied to describe the heat-treatment process for alloys made by laser PBF. As another example, kMC has been adopted to simulate the grain growth in friction-based solid-state MAM processes [112, 113]. Generally, inputs to late-time models are the as-built microstructures generated from the solidification models.

## 7 Processes unique to solid-state AM

As mentioned earlier, there are four solid-state AM techniques: cold spray, friction-based AM, field-assisted AM, and binder jetting.

**Fig. 6** PF simulations and experimental images of AMed Inconel 718 before and after homogenization at a temperature of 1080°C. Reproduced from Ref. [114], which is under CC BY



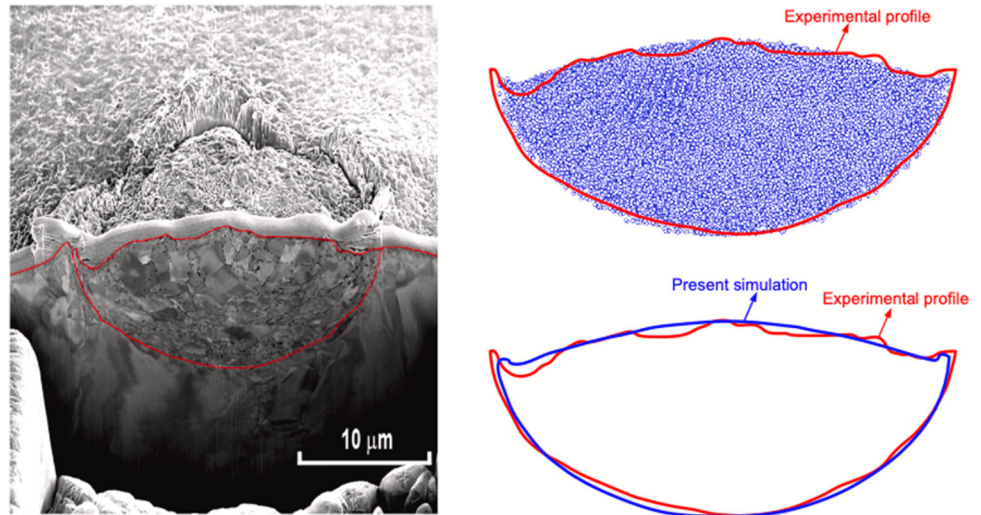
In cold spray, powdered metals are accelerated at high velocities onto substrates without melting. SPH has been employed to simulate the cold spray AM process involving multi-layer multi-track powders [115]. This mesh-free approach, enhanced by kernel gradient correction, adaptive smoothing length, and a constitutive model, adeptly handles large deformations and moving interfaces typical in cold spray processes. The use of SPH, inherently suited for capturing discontinuities such as voids during high-velocity impacts, provides a robust framework for modeling complex physical phenomena, including phase changes and jet formations at the substrate-powder interfaces. The experimental and simulation results are compared in Fig. 7.

There are three stand-alone field-assisted MAM processes, based on electric field, acoustic field, and thermal field, respectively [116]. To our best knowledge, no physics models have been developed or applied to any of them. However, physics models have been employed to simulate these fields when they were used as auxiliary fields to aid in melt-based AM processes [117]. For example, in DED, acoustic and thermal fields, respectively, have been simulated using VOF [118, 119] and FEM [120, 121]. We emphasize that those AM processes are melt-based instead of solid-state.

In friction-based AM processes, metals are joined and built up by using frictional heat generated through mechanical rubbing, which softens the materials without fully melting them. The AFS-D process has been simulated using SPH [57, 58]. This approach employs a fully coupled thermo-



**Fig. 7** Comparisons between experimental observation and simulation for the spraying of a Cu powder. Reproduced with permission from Ref. [115]



mechanical model to handle the substantial plastic deformation and thermal gradients due to frictional heat. As shown in Fig. 8, different actuator feed rates lead to different temperature contours.

In binder jetting, a liquid binding agent is selectively deposited onto a powder bed layer by layer to bond the powder particles and form a solid part. Tan [122] employed a Cartesian grid-based VOF method to study the impact of penetration of micrometer-sized droplets on a powder bed. The physics-based model accurately tracks the interface between the liquid and air during the impact, by integrating a contact angle model to account for the wetting effects on the powder particles.

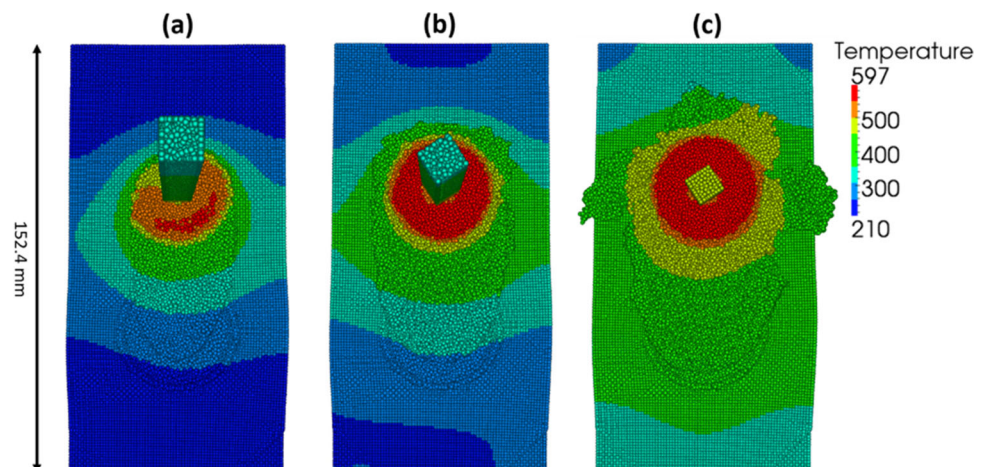
Once a material is made by binder jetting, it is usually sintered to fuse particles together, thereby increasing the material's density and mechanical strength by reducing porosity and creating solid, interconnected bonds between the powder particles. The densification process in sintering has been simulated by FEM [123], which incorporates material properties such as viscosity, creep parameters, and

thermal-mechanical properties dependent on relative density and temperature. Predictions based on the FEM model aligned well with experimental observations [124, 125].

## 8 Conclusions and perspectives

Melt-based and solid-state MAM processes underscore the transformative potential of these technologies in shaping the future of industrial manufacturing. While both MAM techniques offer distinct advantages — melt-based MAM for its precision in creating complex geometries and solid-state MAM for its superior mechanical properties and reduced residual stress — the choice between them depends largely on the specific application requirements and the inherent material characteristics. As MAM continues to evolve, the employment of advanced computational models is crucial

**Fig. 8** Temperature (in °C) contours in AFS-D corresponding to different actuator feed rates: **a** 63.5 mm/min, **b** 127 mm/min, and **c** 254 mm/min. Reproduced with permission from Ref. [58]





for enhancing the predictability and reliability of these processes. The present review of those models not only helps in understanding the intricate microstructural evolution during and post-manufacturing but also aids in optimizing process parameters to mitigate defects and enhance material properties.

Looking forward, the ongoing development and refinement of these computational tools will play a pivotal role in overcoming current limitations related to material properties, process stability, and cost-effectiveness. Moreover, as industry and academia push the boundaries of what's possible with MAM, continued collaboration and knowledge exchange will be vital. Open-source software and community-driven innovations will likely lead to more accessible and versatile MAM solutions, broadening the scope of applications across sectors such as aerospace, automotive, and biomedical. Ultimately, the future of MAM is not only about refining the processes and materials but also about integrating these advancements into a sustainable manufacturing paradigm that aligns with global economic and environmental goals.

Integrating physics-based process models with models that elucidate the structure–property relation is essential for comprehending the entire process–structure–property continuum in MAM. This integration enables a holistic understanding of how variations in manufacturing parameters influence microstructural features, and subsequently, how these microstructures determine the mechanical properties of the final product. Such models help in predicting and optimizing the properties of manufactured parts by enabling simulations that adjust processing conditions to achieve desired outcomes. For example, adjusting heat power and scan speed in melt-based MAM can be simulated to predict changes in grain size and orientation, which directly impact the metal's strength and fatigue resistance. Ultimately, this comprehensive modeling approach is fundamental for advancing MAM technologies, allowing for the precise tailoring of materials to meet specific performance criteria, and facilitating the development of next-generation alloys with optimized properties.

**Author contribution** SX and YS conceptualized the review article. SX and MYA wrote the first draft of the manuscript. All authors revised the manuscript and approved the final manuscript.

**Funding** This research was supported by seed funding from the University of Oklahoma (OU) Data Institute for Societal Challenges. Additionally, MYA and SX are grateful for the startup funds provided by OU. YS was supported in part through the Utah NASA Space Grant Consortium, NASA Grant #80NSSC20M0103.

## Declarations

**Conflict of interest** The authors declare no competing interests.

## References

- Amzallag N (2009) From metallurgy to Bronze age civilizations: the synthetic theory. *Am J Archaeol* 113(4):497–519. <https://doi.org/10.3764/aja.113.4.497>
- Lee C, Maresca F, Feng R, Chou Y, Ungar T, Widom M, An K, Poplawsky JD, Chou Y-C, Liaw PK, Curtin WA (2021) Strength can be controlled by edge dislocations in refractory high-entropy alloys. *Nat Comm* 12(1):5474. <https://doi.org/10.1038/s41467-021-25807-w>
- Zhang W, Xu J (2022) Advanced lightweight materials for automobiles: a review. *Mater Des* 221:110994. <https://doi.org/10.1016/j.matdes.2022.110994>
- Egner H, Skoczeń B (2010) Ductile damage development in two-phase metallic materials applied at cryogenic temperatures. *Int J Plast* 26(4):488–506. <https://doi.org/10.1016/j.ijplas.2009.08.006>
- Eswarappa Prameela S, Pollock TM, Raabe D, Meyers MA, Aitkaliyeva A, Chintersingh K-L, Cordero ZC, Graham-Brady L (2023) Materials for extreme environments. *Nat Rev Mater* 8(2):81–88. <https://doi.org/10.1038/s41578-022-00496-z>
- Frazier WE (2014) Metal additive manufacturing: a review. *J Mater Eng Perform* 23(6):1917–1928. <https://doi.org/10.1007/s11665-014-0958-z>
- Bandyopadhyay A, Traxel KD, Lang M, Juhasz M, Eliaz N, Bose S (2022) Alloy design via additive manufacturing: advantages, challenges, applications and perspectives. *Mater Today* 52:207–224. <https://doi.org/10.1016/j.mattod.2021.11.026>
- Javaid M, Haleem A, Singh RP, Suman R, Rab S (2021) Role of additive manufacturing applications towards environmental sustainability. *Adv Ind Eng Polym Res* 4(4):312–322. <https://doi.org/10.1016/j.aiepr.2021.07.005>
- Lewandowski JJ, Seifi M (2016) Metal additive manufacturing: a review of mechanical properties. *Ann Rev Mater Res* 46:151–186. <https://doi.org/10.1146/annurev-matsci-070115-032024>
- Vafadar A, Guzzomi F, Rassau A, Hayward K (2021) Advances in metal additive manufacturing: a review of common processes, industrial applications, and current challenges. *Appl Sci* 11(3):1213. <https://doi.org/10.3390/app11031213>
- DeRoy T, Wei HL, Zuback JS, Mukherjee T, Elmer JW, Milewski JO, Beese AM, Wilson-Heid Ad, De A, Zhang W (2018) Additive manufacturing of metallic components—process, structure and properties. *Progress Mater Sci* 92:112–224
- Mukherjee T, Zuback J, De A, DeRoy T (2016) Printability of alloys for additive manufacturing. *Sci Rep* 6(1):19717
- Palanivel S, Nelaturu P, Glass B, Mishra RS (2015) Friction stir additive manufacturing for high structural performance through microstructural control in an mg based we43 alloy. *Mater Des* 1980–2015(65):934–952
- Moridi A, Stewart EJ, Wakai A, Assadi H, Gartner F, Guagliano M, Klassen T, Dao M (2020) Solid-state additive manufacturing of porous ti-6al-4v by supersonic impact. *Appl Mater Today* 21:100865
- Wang L, Guo Q, Chen L, Yan W (2023) In-situ experimental and high-fidelity modeling tools to advance understanding of metal additive manufacturing. *Int J Mach Tools Manuf* 193:104077. <https://doi.org/10.1016/j.ijmactools.2023.104077>
- Francois MM, Sun A, King WE, Henson NJ, Tourret D, Bronkhorst CA, Carlson NN, Newman CK, Haut T, Bakosi J, Gibbs JW, Livescu V, Vander Wiel SA, Clarke AJ, Schraad MW, Blacker T, Lim H, Rodgers T, Owen S, Abdeljawad F, Madison J, Anderson AT, Fattebert J-L, Ferencz RM, Hodge NE, Khairallah SA, Walton O (2017) Modeling of additive manufacturing processes for metals: challenges and opportunities. *Curr Opin Solid*

- State Mater Sci 21(4):198–206. <https://doi.org/10.1016/j.cossms.2016.12.001>
17. Smith J, Xiong W, Yan W, Lin S, Cheng P, Kafka OL, Wagner GJ, Cao J, Liu WK (2016) Linking process, structure, property, and performance for metal-based additive manufacturing: computational approaches with experimental support. *Comput Mech* 57(4):583–610. <https://doi.org/10.1007/s00466-015-1240-4>
  18. Yan W, Lian Y, Yu C, Kafka OL, Liu Z, Liu WK, Wagner GJ (2018) An integrated process-structure-property modeling framework for additive manufacturing. *Comput Meth Appl Mech Eng* 339:184–204. <https://doi.org/10.1016/j.cma.2018.05.004>
  19. Michopoulos JG, Iliopoulos AP, Steuben JC, Birnbaum AJ, Lambrakos SG (2018) On the multiphysics modeling challenges for metal additive manufacturing processes. *Addit Manuf* 22:784–799. <https://doi.org/10.1016/j.addma.2018.06.019>
  20. Herriott C, Li X, Kouraytem N, Tari V, Tan W, Anglin B, Rollett AD, Spear AD (2019) A multi-scale, multi-physics modeling framework to predict spatial variation of properties in additive-manufactured metals. *Modelling Simul Mater Sci Eng* 27(2):025009. <https://doi.org/10.1088/1361-651X/aaf753>
  21. Khanafer K, Al-Masri A, Aithal S, Deiab I (2019) Multiphysics modeling and simulation of laser additive manufacturing process. *Int J Interact Des Manuf* 13(2):537–544. <https://doi.org/10.1007/s12008-018-0520-6>
  22. Tan W, Spear A (2024) Multiphysics modeling framework to predict process-microstructure-property relationship in fusion-based metal additive manufacturing. *Acc Mater Res* 5(1):10–21. <https://doi.org/10.1021/accounts.mr.3c00108>
  23. Sharma S, Joshi SS, Pantawane MV, Radhakrishnan M, Mazumder S, Dahotre NB (2023) Multiphysics multi-scale computational framework for linking process-structure-property relationships in metal additive manufacturing: a critical review. *Int Mater Rev* 68(7):943–1009. <https://doi.org/10.1080/09506608.2023.2169501>
  24. Babuska TF, Krick BA, Susan DF, Kustas AB (2021) Comparison of powder bed fusion and directed energy deposition for tailoring mechanical properties of traditionally brittle alloys. *Manuf Lett* 28:30–34. <https://doi.org/10.1016/j.mfglet.2021.02.003>
  25. Dev Singh D, Mahender T, Raji Reddy A (2021) Powder bed fusion process: a brief review. *Mater Today Proc* 46:350–355. <https://doi.org/10.1016/j.matpr.2020.08.415>
  26. Ahn D-G (2021) Directed energy deposition (DED) process: state of the art. *Int J Precis Eng Manuf-Green Tech* 8(2):703–742. <https://doi.org/10.1007/s40684-020-00302-7>
  27. Singh A, Kapil S, Das M (2020) A comprehensive review of the methods and mechanisms for powder feedstock handling in directed energy deposition. *Addit Manuf* 35:101388. <https://doi.org/10.1016/j.addma.2020.101388>
  28. Lee J, Kim K, Choi J, Kim JG, Kim S (2023) Comparative study on fatigue crack propagation behavior of Ti-6Al-4V products made by DED (direct energy deposition) and L-PBF (laser-powder bed fusion) process. *J Mater Res Tech* 23:4499–4512. <https://doi.org/10.1016/j.jmrt.2023.02.096>
  29. Koike M, Greer P, Owen K, Lilly G, Murr LE, Gaytan SM, Martinez E, Okabe T (2011) Evaluation of titanium alloys fabricated using rapid prototyping technologies—electron beam melting and laser beam melting. *Materials* 4(10):1776–1792. <https://doi.org/10.3390/ma4101776>
  30. Tuncer N, Bose A (2020) Solid-state metal additive manufacturing: a review. *JOM* 72(9):3090–3111. <https://doi.org/10.1007/s11837-020-04260-y>
  31. Vaz RF, Silvello A, Albaladejo V, Sanchez J, Cano IG (2021) Improving the wear and corrosion resistance of maraging part obtained by cold gas spray additive manufacturing. *Metals* 11(7):1092. <https://doi.org/10.3390/met11071092>
  32. Al Noman A, Kumar BK, Dickens T (2023) Field assisted additive manufacturing for polymers and metals: materials and methods. *Virtual Phys Prototyp* 18(1):2256707. <https://doi.org/10.1080/17452759.2023.2256707>
  33. Venkit H, Selvaraj SK (2022) Review on latest trends in friction-based additive manufacturing techniques. *Proc Inst Mech Eng, Part C* 236(18):10090–10121. <https://doi.org/10.1177/09544062221101754>
  34. Lores A, Azurmendi N, Agote In, Zuza E (2019) A review on recent developments in binder jetting metal additive manufacturing: materials and process characteristics. *Powder Metall.* 62(5):267–296. 10.1080/00325899.2019.1669299
  35. Habiba U, Hebert RJ (2023) Powder spreading mechanism in laser powder bed fusion additive manufacturing: experiments and computational approach using discrete element method. *Materials* 16(7):2824. <https://doi.org/10.3390/ma16072824>. Accessed 12 Apr 2024
  36. Munagala VNV, Akinyi V, Vo P, Chromik RR (2018) Influence of powder morphology and microstructure on the cold spray and mechanical properties of Ti6Al4V coatings. *J Therm Spray Tech* 27(5):827–842. <https://doi.org/10.1007/s11666-018-0729-8>. Accessed 12 Apr 2024
  37. Bhavsar S, James S (2018) Thermo-mechanical finite element analysis of ultrasonic powder consolidation process. *Addit Manuf* 21:705–712. <https://doi.org/10.1016/j.addma.2018.04.021>. Accessed 12 Apr 2024
  38. Miyanaji H, Rahman KM, Da M, Williams CB (2020) Effect of fine powder particles on quality of binder jetting parts. *Addit. Manuf.* 36:101587. <https://doi.org/10.1016/j.addma.2020.101587>. Accessed 12 Apr 2024
  39. Qiu C, Panwisawas C, Ward M, Basoalto HC, Brooks JW, Attallah MM (2015) On the role of melt flow into the surface structure and porosity development during selective laser melting. *Acta Mater* 96:72–79. <https://doi.org/10.1016/j.actamat.2015.06.004>. Accessed 12 Apr 2024
  40. Körner C, Bauereiß A, Attar E (2013) Fundamental consolidation mechanisms during selective beam melting of powders. *Modelling Simul Mater Sci Eng* 21(8):085011. <https://doi.org/10.1088/0965-0393/21/8/085011>. Accessed 12 Apr 2024
  41. Bhalode P, Ierapetritou M (2020) Discrete element modeling for continuous powder feeding operation: calibration and system analysis. *Int J Pharm* 585:119427. <https://doi.org/10.1016/j.ijpharm.2020.119427>. Accessed 12 Apr 2024
  42. Chen H, Sun Y, Yuan W, Pang S, Yan W, Shi Y (2022) A review on discrete element method simulation in laser powder bed fusion additive manufacturing. *Chin J Mech Eng Addit Manuf Front* 1(1):100017. <https://doi.org/10.1016/j.cjmeam.2022.100017>. Accessed 12 Apr 2024
  43. Fletcher DF, Chaugule V, Reis L, Young PM, Traini D, Soria J (2021) On the use of computational fluid dynamics (CFD) modelling to design improved dry powder inhalers. *Pharm Res* 38(2):277–288. <https://doi.org/10.1007/s11095-020-02981-y>. Accessed 12 Apr 2024
  44. Rosemann T, Kravets B, Reinecke SR, Kruggel-Emden H, Wu M, Peters B (2019) Comparison of numerical schemes for 3D lattice Boltzmann simulations of moving rigid particles in thermal fluid flows. *Powder Tech* 356:528–546. <https://doi.org/10.1016/j.powtec.2019.07.054>. Accessed 12 Apr 2024
  45. Booth RA, Sijacki D, Clarke CJ (2015) Smoothed particle hydrodynamics simulations of gas and dust mixtures. *Mon Not R Astron Soc* 452(4):3932–3947. <https://doi.org/10.1093/mnras/stv1486>. Accessed 12 Apr 2024
  46. Tan JH, Wong WLE, Dalgarno KW (2017) An overview of powder granulometry on feedstock and part performance in the selective laser melting process. *Addit Manuf* 18:228–255. <https://doi.org/10.1016/j.addma.2017.10.011>. Accessed 12 Apr 2024

47. Lampitella V, Trofa M, Astarita A, D'Avino G (2021) Discrete element method analysis of the spreading mechanism and its influence on powder bed characteristics in additive manufacturing. *Micromachines* 12(4):392. <https://doi.org/10.3390/mi12040392>. Accessed 12 Apr 2024
48. Parry L, Ashcroft IA, Wildman RD (2016) Understanding the effect of laser scan strategy on residual stress in selective laser melting through thermo-mechanical simulation. *Addit Manuf* 12:1–15. <https://doi.org/10.1016/j.addma.2016.05.014>. Accessed 30 Apr 2024
49. Geer S, Bernhardt-Barry ML, Garboczi EJ, Whiting J, Donmez A (2018) A more efficient method for calibrating discrete element method parameters for simulations of metallic powder used in additive manufacturing. *Granular Matter* 20(4):77. <https://doi.org/10.1007/s10035-018-0848-4>. Accessed 28 Apr 2024
50. Dosta M, Andre D, Angelidakis V, Caulk RA, Celigueta MA, Chareyre B, Dietiker J-F, Girardot J, Govender N, Hubert C, Kobyłka R, Moura AF, Skorych V, Weatherley DK, Weinhart T (2024) Comparing open-source DEM frameworks for simulations of common bulk processes. *Comput Phys Comm* 296:109066. <https://doi.org/10.1016/j.cpc.2023.109066>. Accessed 28 Apr 2024
51. André D, Charles J-L, Iordanoff I, Néauport J (2014) The GranOO workbench, a new tool for developing discrete element simulations, and its application to tribological problems. *Adv. Eng. Software* 74:40–48. <https://doi.org/10.1016/j.advengsoft.2014.04.003>. Accessed 28 Apr 2024
52. Dadvand P, Rossi R, Oñate E (2010) An object-oriented environment for developing finite element codes for multi-disciplinary applications. *Arch Comput Methods Eng* 17(3):253–297. <https://doi.org/10.1007/s11831-010-9045-2>. Accessed 28 Apr 2024
53. Weinhart T, Orefice L, Post M, Schroyen Lantman MP, Denisson IFC, Tunuguntla DR, Tsang JMF, Cheng H, Shaheen MY, Shi H, Rapino P, Grannonio E, Losacco N, Barbosa J, Jing L, Alvarez Naranjo JE, Roy S, Otter WK, Thornton AR (2020) Fast, flexible particle simulations — an introduction to MercuryDPM. *Comput Phys Comm* 249, 107129. <https://doi.org/10.1016/j.cpc.2019.107129>. Accessed 28 Apr 2024
54. Dosta M, Skorych V (2020) MUSEN: an open-source framework for GPU-accelerated DEM simulations. *SoftwareX* 12:100618. <https://doi.org/10.1016/j.softx.2020.100618>. Accessed 28 Apr 2024
55. Smilauer V, Angelidakis V, Catalano E, Caulk R, Chareyre B, Chèvremont W, Dorofeenko S, Duriez J, Dyck N, Elias J, Er B, Eulitz A, Gladky A, Guo N, Jakob C, Kneib F, Kozicki J, Marzougui D, Maurin R, Modenese C, Pekmezci G, Scholtès L, Sibille L, Stransky J, Sweijen T, Thoeni K, Yuan C (2021) Yade documentation. The Yade Project. <https://doi.org/10.5281/zenodo.5705394>. Version Number: 3rd. <https://zenodo.org/records/5705394>. Accessed 28 Apr 2024
56. Barath Kumar MD, Manikandan M (2022) Assessment of process, parameters, residual stress mitigation, post treatments and finite element analysis simulations of wire arc additive manufacturing technique. *Met Mater Int* 28(1):54–111. <https://doi.org/10.1007/s12540-021-01015-5>. Accessed 12 Apr 2024
57. Yang HG (2020) Numerical simulation of the temperature and stress state on the additive friction stir with the smoothed particle hydrodynamics method. *Strength Mater* 52(1):24–31. <https://doi.org/10.1007/s11223-020-00146-1>. Accessed 12 Apr 2024
58. Stubblefield GG, Fraser K, Phillips BJ, Jordon JB, Allison PG (2021) A meshfree computational framework for the numerical simulation of the solid-state additive manufacturing process, additive friction stir-deposition (AFS-D). *Mater Des* 202:109514. <https://doi.org/10.1016/j.matdes.2021.109514>. Accessed 12 Apr 2024
59. Bayat M, Nadimpalli VK, Biondani FG, Jafarzadeh S, Thorborg J, Tiedje NS, Bissacco G, Pedersen DB, Hattel JH (2021) On the role of the powder stream on the heat and fluid flow conditions during Directed Energy Deposition of maraging steel – multiphysics modeling and experimental validation. *Addit Manuf* 43:102021. <https://doi.org/10.1016/j.addma.2021.102021>. Accessed 28 Apr 2024
60. Jiang H-Z, Li Z-Y, Feng T, Wu P-Y, Chen Q-S, Feng Y-L, Chen L-F, Hou J-Y, Xu H-J (2021) Effect of process parameters on defects, melt pool shape, microstructure, and tensile behavior of 316L stainless steel produced by selective laser melting. *Acta Metall Sin (Engl Lett)* 34(4):495–510. <https://doi.org/10.1007/s40195-020-01143-8>. Accessed 28 Apr 2024
61. Kiss AM, Fong AY, Calta NP, Thampy V, Martin AA, Depond PJ, Wang J, Matthews MJ, Ott RT, Tassone CJ, Stone KH, Kramer MJ, Buuren A, Toney MF, Nelson Weker J (2019) Laser-induced keyhole defect dynamics during metal additive manufacturing. *Adv Eng Mater* 21(10):1900455. <https://doi.org/10.1002/adem.201900455>. Accessed 28 Apr 2024
62. Mojumder S, Gan Z, Li Y, Amin AA, Liu WK (2023) Linking process parameters with lack-of-fusion porosity for laser powder bed fusion metal additive manufacturing. *Addit Manuf* 68:103500. <https://doi.org/10.1016/j.addma.2023.103500>. Accessed 28 Apr 2024
63. Guo C, Li G, Li S, Hu X, Lu H, Li X, Xu Z, Chen Y, Li Q, Lu J, Zhu Q (2023) Additive manufacturing of Ni-based superalloys: residual stress, mechanisms of crack formation and strategies for crack inhibition. *Nano Mater Sci* 5(1):53–77. <https://doi.org/10.1016/j.nanoms.2022.08.001>. Accessed 28 Apr 2024
64. Cao Y, Lin X, Kang N, Ma L, Wei L, Zheng M, Yu J, Peng D, Huang W (2021) A novel high-efficient finite element analysis method of powder bed fusion additive manufacturing. *Addit Manuf* 46:102187. <https://doi.org/10.1016/j.addma.2021.102187>. Accessed 28 Apr 2024
65. Cattenone A, Morganti S, Auricchio F (2020) Basis of the lattice Boltzmann method for additive manufacturing. *Arch Comput Methods Eng* 27(4):1109–1133. <https://doi.org/10.1007/s11831-019-09347-7>. Accessed 28 Apr 2024
66. Lüthi C, Afrasiabi M, Bambach M (2023) An adaptive smoothed particle hydrodynamics (SPH) scheme for efficient melt pool simulations in additive manufacturing. *Comput Math Appl* 139:7–27. <https://doi.org/10.1016/j.camwa.2023.03.003>. Accessed 28 Apr 2024
67. Li M-J, Chen J, Lian Y, Xiong F, Fang D (2023) An efficient and high-fidelity local multi-mesh finite volume method for heat transfer and fluid flow problems in metal additive manufacturing. *Comput Meth Appl Mech Eng* 404:115828. <https://doi.org/10.1016/j.cma.2022.115828>. Accessed 28 Apr 2024
68. Ye Q, Chen S (2017) Numerical modeling of metal-based additive manufacturing using level set methods. *J Manuf Sci Eng* 139(071019). <https://doi.org/10.1115/1.4036290>. Accessed 28 Apr 2024
69. Aidun CK, Clausen JR (2010) Lattice-Boltzmann method for complex flows. *Ann Rev Fluid Mech* 42:439–472. <https://doi.org/10.1146/annurev-fluid-121108-145519>. Accessed 28 Apr 2024
70. Lind SJ, Rogers BD, Stansby PK (2020) Review of smoothed particle hydrodynamics: towards converged Lagrangian flow modelling. *Proc R Soc A* 476(2241):20190801. <https://doi.org/10.1098/rspa.2019.0801>. Accessed 28 Apr 2024
71. Acharya S, Baliga BR, Karki K, Murthy JY, Prakash C, Vanka SP (2007) Pressure-based finite-volume methods in computational fluid dynamics. *J Heat Mass Transf* 129(4):407–424. <https://doi.org/10.1115/1.2716419>. Accessed 28 Apr 2024
72. Yang R, Chen W, Tang L, Ma J, Zhou Q, Lei X, Yao W, Wang N (2023) Research on the melt pool shape formation mechanism of the laser surface remelting of nickel-based single-crystal super-



- alloy. *Curr Comput-Aided Drug Des* 13(8):1162. <https://doi.org/10.3390/cryst13081162>. Accessed 1 May 2024
73. Mishra AK, Kumar A (2024) Effect of process parameters on melt pool characteristics and solidification process during laser powder bed fusion of AlSi10Mg alloy. *Lasers Manuf Mater Process*. <https://doi.org/10.1007/s40516-023-00243-4>. Accessed 1 May 2024
  74. Ou W, Mukherjee T, Knapp GL, Wei Y, DebRoy T (2018) Fusion zone geometries, cooling rates and solidification parameters during wire arc additive manufacturing. *Int J Heat Mass Transf* 127:1084–1094. <https://doi.org/10.1016/j.ijheatmasstransfer.2018.08.111>. Accessed 28 Apr 2024
  75. Wang L, Zhang Y, Yan W (2020) Evaporation model for key-hole dynamics during additive manufacturing of metal. *Phys Rev Appl* 14(6):064039. <https://doi.org/10.1103/PhysRevApplied.14.064039>. Accessed 28 Apr 2024
  76. Wang Q, Li M, Xu W, Yao L, Liu X, Su D, Wang P (2020) Review on liquid film flow and heat transfer characteristics outside horizontal tube falling film evaporator: CFD numerical simulation. *Int J Heat Mass Transf* 163:120440. <https://doi.org/10.1016/j.ijheatmasstransfer.2020.120440>. Accessed 28 Apr 2024
  77. Lamnatou C, Papanicolaou E, Belessiotis V, Kyriakis N (2010) Finite-volume modelling of heat and mass transfer during convective drying of porous bodies – non-conjugate and conjugate formulations involving the aerodynamic effects. *Renewable Energy* 35(7):1391–1402. <https://doi.org/10.1016/j.renene.2009.11.008>. Accessed 28 Apr 2024
  78. Diaz-Damacillo L, Sigalotti LDG, Alvarado-Rodríguez CE, Klapp J (2023) Smoothed particle hydrodynamics simulations of the evaporation of suspended liquid droplets. *Phys Fluids* 35(12):122111. <https://doi.org/10.1063/5.0176846>. Accessed 28 Apr 2024
  79. Oñate E, Rojek J (2004) Combination of discrete element and finite element methods for dynamic analysis of geomechanics problems. *Comput Methods Appl Mech Eng* 193(27):3087–3128. <https://doi.org/10.1016/j.cma.2003.12.056>. Accessed 28 Apr 2024
  80. Wang D, Wu S, Fu F, Mai S, Yang Y, Liu Y, Song C (2017) Mechanisms and characteristics of spatter generation in SLM processing and its effect on the properties. *Mater Des* 117:121–130. <https://doi.org/10.1016/j.matdes.2016.12.060>. Accessed 28 Apr 2024
  81. Mahmoudi M, Tapia G, Karayagiz K, Franco B, Ma J, Arroyave R, Karaman I, Elwany A (2018) Multivariate calibration and experimental validation of a 3D finite element thermal model for laser powder bed fusion metal additive manufacturing. *Integr Mater Manuf Innov* 7(3):116–135. <https://doi.org/10.1007/s40192-018-0113-z>. Accessed 29 Apr 2024
  82. Coleman J, Plotkowski A, Stump B, Raghavan N, Sabau AS, Krane MJM, Heigel J, Ricker RE, Levine L, Babu SS (2020) Sensitivity of thermal predictions to uncertain surface tension data in laser additive manufacturing. *J Heat Transf* 142(12):122201. <https://doi.org/10.1115/1.4047916>. Accessed 15 Apr 2024
  83. Weller HG, Tabor G, Jasak H, Fureby C (1998) A tensorial approach to computational continuum mechanics using object-oriented techniques. *Comput Phys* 12(6):620–631. <https://doi.org/10.1063/1.168744>. Accessed 29 Apr 2024
  84. Carlson N (2024) Truchas-PBF / truchas-pbf · GitLab. <https://gitlab.com/truchas-pbf/truchas-pbf>. Accessed 29 Apr 2024
  85. Korzekwa DA (2009) Truchas – a multi-physics tool for casting simulation. *Int J Cast Metals Res* 22(1–4):187–191. <https://doi.org/10.1179/136404609X367641>. Accessed 29 Apr 2024
  86. Alnæs M, Blechta J, Hake J, Johansson A, Kehlet B, Logg A, Richardson C, Ring J, Rognes ME, Wells GN (2015) The FEniCS project version 1.5. *Archive of Numerical Software* 3(100). <https://doi.org/10.11588/ans.2015.100.20553>. Accessed 29 Apr 2024
  87. Latt J, Malaspinas O, Kontaxakis D, Parmigiani A, Lagrava D, Brogi F, Belgacem MB, Thorimbert Y, Leclaire S, Li S, Marson F, Lemus J, Kotsalos C, Conradin R, Coreixas C, Petkantchin R, Raynaud F, Beny J, Chopard B (2021) Palabos: parallel lattice Boltzmann solver. *Comput Math Appl* 81:334–350. <https://doi.org/10.1016/j.camwa.2020.03.022>. Accessed 29 Apr 2024
  88. Crespo AJC, Domínguez JM, Rogers BD, Gómez-Gesteira M, Longshaw S, Canelas R, Vacondio R, Barreiro A, García-Feal O (2015) DualSPHysics: open-source parallel CFD solver based on Smoothed Particle Hydrodynamics (SPH). *Comput Phys Comm* 187:204–216. <https://doi.org/10.1016/j.cpc.2014.10.004>. Accessed 29 Apr 2024
  89. Körner C, Markl M, Koepf JA (2020) Modeling and simulation of microstructure evolution for additive manufacturing of metals: a critical review. *Metall Mater Trans A* 51(10):4970–4983. <https://doi.org/10.1007/s11661-020-05946-3>. Accessed 28 Apr 2024
  90. Dogu MN, McCarthy E, McCann R, Mahato V, Caputo A, Bambach M, Ahad IU, Brabazon D (2022) Digitisation of metal AM for part microstructure and property control. *Int J Mater Form* 15(3):30. <https://doi.org/10.1007/s12289-022-01686-4>. Accessed 28 Apr 2024
  91. Karthik GM, Kim HS (2021) Heterogeneous aspects of additive manufactured metallic parts: a review. *Met Mater Int* 27(1):1–39. <https://doi.org/10.1007/s12540-020-00931-2>. Accessed 28 Apr 2024
  92. Stump B, Plotkowski A, Coleman J (2021) Solidification dynamics in metal additive manufacturing: analysis of model assumptions. *Modelling Simul Mater Sci Eng* 29(3):035001. <https://doi.org/10.1088/1361-651X/abca19>. Accessed 28 Apr 2024
  93. Kotas P, Tutum CC, Thorborg J, Hattel JH (2012) Elimination of hot tears in steel castings by means of solidification pattern optimization. *Metall Mater Trans B* 43(3):609–626. <https://doi.org/10.1007/s11663-011-9617-z>. Accessed 28 Apr 2024
  94. Rolchigo M, Reeve ST, Stump B, Knapp GL, Coleman J, Plotkowski A, Belak J (2022) ExaCA: a performance portable exascale cellular automata application for alloy solidification modeling. *Comput. Mater. Sci.* 214:111692. <https://doi.org/10.1016/j.commatsci.2022.111692>. Accessed 16 Apr 2024
  95. Sahoo S, Chou K (2016) Phase-field simulation of microstructure evolution of Ti-6Al-4V in electron beam additive manufacturing process. *Addit Manuf* 9:14–24. <https://doi.org/10.1016/j.addma.2015.12.005>. Accessed 5 May 2024
  96. Shan X, Pan Z, Gao M, Han L, Choi J-P, Zhang H (2024) Multi-physics modeling of melting-solidification characteristics in laser powder bed fusion process of 316L stainless steel. *Materials* 17(4):946. <https://doi.org/10.3390/ma17040946>. Accessed 28 Apr 2024
  97. Boettinger WJ, Warren JA, Beckermann C, Karma A (2002) Phase-field simulation of solidification. *Ann Rev Mater Res* 32:163–194. <https://doi.org/10.1146/annurev.matsci.32.101901.155803>. Accessed 29 Apr 2024
  98. Rodgers TM, Madison JD, Tikare V (2017) Simulation of metal additive manufacturing microstructures using kinetic Monte Carlo. *Comput Mater Sci* 135:78–89. <https://doi.org/10.1016/j.commatsci.2017.03.053>. Accessed 29 Apr 2024
  99. Lian Y, Lin S, Yan W, Liu WK, Wagner GJ (2018) A parallelized three-dimensional cellular automaton model for grain growth during additive manufacturing. *Comput Mech* 61(5):543–558. <https://doi.org/10.1007/s00466-017-1535-8>. Accessed 29 Apr 2024
  100. Wang G-X, Matthes EF (1996) Modeling of nonequilibrium surface melting and resolidification for pure metals and binary alloys. *J Heat Mass Transf* 118(4):944–951. <https://doi.org/10.1115/1.2822593>. Accessed 29 Apr 2024
  101. Miettinen J (2006) Thermodynamic-kinetic model for the simulation of solidification in binary copper alloys and calculation

- of thermophysical properties. *Comput Mater Sci* 36(4):367–380. <https://doi.org/10.1016/j.commatsci.2005.05.004>. Accessed 29 Apr 2024
102. Grafe U, Böttger B, Tiaden J, Fries SG (2000) Coupling of multicomponent thermodynamic databases to a phase field model: application to solidification and solid state transformations of superalloys. *Scr Mater* 42(12):1179–1186. [https://doi.org/10.1016/S1359-6462\(00\)00355-9](https://doi.org/10.1016/S1359-6462(00)00355-9). Accessed 29 Apr 2024
  103. Sargent N, Jones M, Otis R, Shapiro AA, Delplanque J-P, Xiong W (2021) Integration of processing and microstructure models for non-equilibrium solidification in additive manufacturing. *Metals* 11(4):570. <https://doi.org/10.3390/met11040570>. Accessed 29 Apr 2024
  104. Ghosh S, Newman CK, Francois MM (2022) Tusas: a fully implicit parallel approach for coupled phase-field equations. *J Comput Phys* 448:110734. <https://doi.org/10.1016/j.jcp.2021.110734>. Accessed 15 Apr 2024
  105. Dorr MR, Fattebert J-L, Wickett ME, Belak JF, Turchi PEA (2010) A numerical algorithm for the solution of a phase-field model of polycrystalline materials. *J Comput Phys* 229(3):626–641. <https://doi.org/10.1016/j.jcp.2009.09.041>. Accessed 29 Apr 2024
  106. Mitchell JA, Abdeljawad F, Battaile C, Garcia-Cardona C, Holm EA, Homer ER, Madison J, Rodgers TM, Thompson AP, Tikare V, Webb E, Plimpton SJ (2023) Parallel simulation via SPPARKS of on-lattice kinetic and Metropolis Monte Carlo models for materials processing. *Modelling Simul Mater Sci Eng* 31(5):055001. <https://doi.org/10.1088/1361-651X/accc4b>. Accessed 29 Apr 2024
  107. Lu Z, Xue X, Meng L, Zeng Q, Chi Y, Fan G, Li H, Zhang Z, Nie F, Zhang C (2017) Heat-induced solid–solid phase transformation of TKX-50. *J Phys Chem C* 121(15):8262–8271. <https://doi.org/10.1021/acs.jpcc.7b00086>. Accessed 29 Apr 2024
  108. Yao XX, Gao X, Zhang Z (2022) Three-dimensional microstructure evolution of Ti-6Al-4V during multi-layer printing: a phase-field simulation. *J Mater Res Tech* 20:934–949. <https://doi.org/10.1016/j.jmrt.2022.07.101>. Accessed 29 Apr 2024
  109. Vilario T, Colin C, Bartout JD (2011) As-fabricated and heat-treated microstructures of the Ti-6Al-4V alloy processed by selective laser melting. *Metall Mater Trans A* 42(10):3190–3199. <https://doi.org/10.1007/s11661-011-0731-y>. Accessed 29 Apr 2024
  110. Ghorbanpour S, Deshmukh K, Sahu S, Riemsag T, Reinton E, Borisov E, Popovich A, Bertolo V, Jiang Q, Sanchez MT, Knezevic M, Popovich V (2022) Additive manufacturing of functionally graded inconel 718: effect of heat treatment and building orientation on microstructure and fatigue behaviour. *J Mater Process Tech* 306:117573. <https://doi.org/10.1016/j.jmatprotec.2022.117573>. Accessed 29 Apr 2024
  111. Radhakrishnan B, Gorti S, Babu SS (2016) Phase field simulations of autocatalytic formation of alpha lamellar colonies in Ti-6Al-4V. *Metall Mater Trans A* 47(12):6577–6592. <https://doi.org/10.1007/s11661-016-3746-6>. Accessed 29 Apr 2024
  112. Wu Q, Zhang Z (2017) Precipitation-induced grain growth simulation of friction-stir-welded AA6082-T6. *J Mater Eng Perform* 26(5):2179–2189. <https://doi.org/10.1007/s11665-017-2639-1>. Accessed 29 Apr 2024
  113. Zhang Z, Hu CP (2018) 3D Monte Carlo simulation of grain growth in friction stir welding. *J Mech Sci Tech* 32(3):1287–1296. <https://doi.org/10.1007/s12206-018-0233-6>. Accessed 29 Apr 2024
  114. Chen M, Du Q, Shi R, Fu H, Liu Z, Xie J (2022) Phase field simulation of microstructure evolution and process optimization during homogenization of additively manufactured Inconel 718 alloy. *Front Mater* 9. <https://doi.org/10.3389/fmats.2022.1043249>. Accessed 6 May 2024
  115. Zhang Z, Shu C, Khalid MSU, Liu Y, Yuan Z, Jiang Q, Liu W (2022) SPH modeling and investigation of cold spray additive manufacturing with multi-layer multi-track powders. *J Manuf Process* 84:565–586. <https://doi.org/10.1016/j.jmapro.2022.10.032>. Accessed 29 Apr 2024
  116. Hu Y (2021) Recent progress in field-assisted additive manufacturing: materials, methodologies, and applications. *Mater Horiz* 8(3):885–911. <https://doi.org/10.1039/D0MH01322F>. Accessed 22 May 2024
  117. Tan C, Li R, Su J, Du D, Du Y, Attard B, Chew Y, Zhang H, Lavernia EJ, Fautrelle Y, Teng J, Dong A (2023) Review on field assisted metal additive manufacturing. *Int J Mach Tools Manuf* 189:104032. <https://doi.org/10.1016/j.ijmachtools.2023.104032>. Accessed 22 May 2024
  118. Yang Z, Wang S, Zhu L, Ning J, Xin B, Dun Y, Yan W (2022) Manipulating molten pool dynamics during metal 3D printing by ultrasound. *Appl Phys Rev* 9(2):021416. <https://doi.org/10.1063/5.0082461>. Accessed 22 May 2024
  119. Ji F, Qin X, Hu Z, Xiong X, Ni M, Wu M (2022) Influence of ultrasonic vibration on molten pool behavior and deposition layer forming morphology for wire and arc additive manufacturing. *Int Comm Heat Mass Transf* 130:105789. <https://doi.org/10.1016/j.icheatmasstransfer.2021.105789>. Accessed 22 May 2024
  120. Dalae MT, Gloor L, Leinenbach C, Wegener K (2020) Experimental and numerical study of the influence of induction heating process on build rates Induction Heating-assisted laser Direct Metal Deposition (IH-DMD). *Surf Coat Tech* 384:125275. <https://doi.org/10.1016/j.surfcoat.2019.125275>. Accessed 22 May 2024
  121. Nie Z, Wang G, McGuffin-Cawley JD, Narayanan B, Zhang S, Schwam D, Kottman M, Rong YK (2016) Experimental study and modeling of H13 steel deposition using laser hot-wire additive manufacturing. *J Mater Process Tech* 235:171–186. <https://doi.org/10.1016/j.jmatprotec.2016.04.006>. Accessed 22 May 2024
  122. Tan H (2016) Three-dimensional simulation of micrometer-sized droplet impact and penetration into the powder bed. *Chem Eng Sci* 153:93–107. <https://doi.org/10.1016/j.ces.2016.07.015>
  123. Zhang K, Zhang W, Brune R, Herderick E, Zhang X, Cornell J, Forsmark J (2021) Numerical simulation and experimental measurement of pressureless sintering of stainless steel part printed by binder jetting additive manufacturing. *Addit Manuf* 47:102330. <https://doi.org/10.1016/j.addma.2021.102330>
  124. Song J, Barriere T, Liu B, Gelin J, Michel G (2010) Experimental and numerical analysis on sintering behaviours of injection moulded components in 316L stainless steel powder. *Powder Metall* 53(4):295–304. <https://doi.org/10.1179/003258908X334212>
  125. Sahli M, Lebid A, Gelin J-C, Barriere T, Necib B (2015) Numerical simulation and experimental analysis of solid-state sintering response of 316 L stainless steel micro-parts manufactured by metal injection molding. *Int J Adv Manuf Tech* 79(9):2079–2092. <https://doi.org/10.1007/s00170-015-6983-8>

**Publisher's Note** Springer Nature remains neutral with regard to jurisdictional claims in published maps and institutional affiliations.

Springer Nature or its licensor (e.g. a society or other partner) holds exclusive rights to this article under a publishing agreement with the author(s) or other rightsholder(s); author self-archiving of the accepted manuscript version of this article is solely governed by the terms of such publishing agreement and applicable law.